Redshift and Mass Determination of a Galaxy Cluster at z∼0.46

Néstor Espinoza, *Undergraduate Student*, PUC

***Abstract*—Using aproximately 120 spectra taken from a group of galaxies using the VLT/FORS2 instrument in The Paranal Observatory, Chile, we present a study of a nearby galaxy cluster. Using visual/automatized line identification and cross-correlation techniques, we measured the redshift of 123 galaxies and formed a velocity distribution that is carefully studied. After careful examination of our data, we detect 83 cluster members on our sample and estimate the cluster's redshift to be $z = 0.462^{+0.0003}_{-0.0004}$. After detecting visual asymmetry in our velocity distribution, we apply a D'Agostino and Pearson's (1973) normality test and reject the hypothesis of a normal distribution which gives rise to the proposition that the cluster may possess departures from equilibrium. We finally estimate the cluster's virial mass to be $M_{200} = \left(9.64^{+1.56}_{-1.58}\right) 10^{14} M_{\odot} h^{-1}$ and discuss whether it is really a massive cluster or an overestimation due to our proposition of non-equilibrium.**

***Index Terms*—Galaxy Clusters, Mass Determination, Virial Theorem, Redshift, Spectroscopy.**

I. Introduction

THE study of the properties of galaxy clusters in modern astrophysics plays a fundamental role on the understanding of large-scale structure formation and evolution. Those properties have been studied by a long time, starting with the pioneering studies by Hubble (1929), who proposed that this large clusters of *nebulae*, as he called them, where apparently receding from us. We now know that these *nebulae* where actually galaxies. Two years later, Hubble & Humason (1931) proved what we today call *Hubble's Law* in a work that included a larger sample of galaxy clusters. As explained, they not only measured the radial velocity of particular galaxies (which they called part of the "local group") but also the radial velocity of clusters of galaxies (determined by the brightest members of the cluster). For this, they measured the *red-shift* of the emission and absorption lines of these objects, estimating indirectly what we today call the *redshift*, z.

Hubble law's linear rationship between distance and velocity could only be explained if the universe where expanding. Thus, knowing the redshift of a cluster of galaxies determines inmediately it's distance from our galaxy with considerable precision (Freedman et al., 2001). However, if we wish to study the structure and evolution of the large-scale structure, we need one more piece of information: The mass of the objects. Mass is one of the most important physical parameters to characterize astrophysical objects. It is not only important for large-scale structure, but also serves as an important constraint on the mass distribution of galaxy clusters, which in turn serves in the study of various fields such as, for example, Galaxy Formation Theory (Benson, 2010) or the recent attempt to build a distribution of Baryonic dark matter in the intracluster medium (Okabe & Umetsu, 2007).

A. Redshift/Velocity estimation of Galaxy Clusters

As explained, by Hubble's law the redshift (and hence the velocity) of the cluster determines it's distance from our galaxy. There are two ways to estimate the cluster's redshift (z). The first is to use the well-known relation between the observed wavelength of emission and/or absorption lines in different galaxies (λ_{obs}) and the wavelength that is measured in the laboratory (λ_{lab}):

$$z = \frac{\lambda_{obs} - \lambda_{lab}}{\lambda_{lab}}$$

Although this is an approximation for low redshifts, it can provide us with enough precision for our study of the galaxy cluster's mass and membership determination.

The second method of redshift estimation is the cross-correlation technique (Tonry & Davis, 1979, hereafter TD79). Basically, the cross-correlation technique takes advantage of our current knowledge of the spectral properties of different galaxies (hereafter the *templates*) and tries to correlate them with our sample spectrum. It assumes that the sample spectrum may be multiplied, shifted (in wavelenght) and/or broadened by a convolution. After removing the continuum from our sample spectrum and from our templates, the cross-correlation algorithm forms a cross-correlation product which gives the form of the cross-corelation function, defined to give a value of 1 if the templates match given the property we want to match (in this case, the redshift). It is important to note that this uses absorption and/or emission lines as well, plus different spectral characteristics present in galaxy spectra (let's remember that, except from the infrared part of the spectrum, galaxies are far from being perfect thermal sources and thus possess unique features that can be compared). As we will see, the cross-correlation technique is a very powerfull method for the estimation of redshift with high precision if treated with care.

Manuscript received October 24, 2010.

N. Espinoza is with the Departamento de Astronomía y Astrofísica, Pontificia Universidad Católica de Chile, Santiago, Chile. Phone: +(56) 09 987749956, e-mail: nsespino@uc.cl.

B. Mass estimation of Galaxy Clusters

According to recent studies, there are three main methods of estimating a cluster's mass observationally. The first method assumes dynamical equilibrium and estimates the cluster's mass via the virial theorem (Girardi et al., 1998, Maurogordato et al., 2008). The second method is based on X-ray observations in which the flux, bolometric luminosity, temperature and metallicity of the source is obtained and fitted to a model. Commonly this assumes hydrostatic equilibrium in the intracluster medium and estimates the masses based on an NFW model fit (Navarro et al., 1996), commonly assumed to be isothermal (Gastaldello et al., 2007). The third method is the method of weak and strong gravitational lensing. This method makes no assumption on the dynamical state of the cluster, so it should (in principle) enable us to determine the gravitational mass directly, as done by Bardac et al. (2006). As proposed in this last work, gravitational lensing not only tell us information about the total mass, but also about the mass distribution of the cluster.

Although there are plenty of ways to estimate a cluster's mass, they do not, in general, agree. For example, Zhang et al. (2010) studies the case of disturbed clusters (i.e. deviations from hydrostatic equilibrium because of, for example, currently forming cluster often called "merging clusters"), and concludes that the mass of the cluster could be both overestimated and underestimated if one compares the results using X-ray observations and the lensing methods, despite the fact that there have been various attempts in solving this problem (see, for example, Allen, 1998, Xiang-Ping Wu, 2000 and H.Y. Shan et al., 2010). Although it is true that we make no dynamical assumptions when determining masses via the weak and strong lensing methods, we do make assumptions on the distribution of mass in the cluster: The determination of mass via this method strongly depends on the line of sight of the lens (for example, imagine that the cluster has an elliptical symmetry: If we look in the semi-mayor axis direction, we'll probably overestimate the mass of the cluster if we assume it to be spherically symmetric). On the other hand, the use of the virial theorem to estimate the cluster's mass can be used if the dyamical state of the cluster is analysed, even if merging events are present, which is done analysing it's velocity distribution (Ferrari et al., 2005). It has been shown that not proving this state can lead to several problems if the cluster has overcome merging events and are not taken in consideration, overestimating it's mass by even a factor of two (M. Takizawa et al., 2010). This can be explained in terms of energies: If one does not account for merging events, the kinetical energy will be overestimated as an equilibrium relation and hence give a bigger mass estimation.

In the present work, we use the mass estimator derived from the virial theorem for a spherically symmetric cluster of galaxies proposed by Calberg et al. (1996, hereafter C96):

$$M_v = \frac{3}{G}\sigma_1^2 r_v$$

Where M_v is the virial mass, σ_1 is the proyected velocity dispersion in the line of sight and r_v is the virial radius, the radius that encloses M_v. Although there are apparently "better" estimators (J.N. Bahcall & S. Tremaine et al, 1981), we'll use this relation mainly because in the present work we don't calculate the spatial distribution of the cluster members, so this method will serve as a good estimator given that it's sensitivity is not dominated by spatial distribution. The problem now is to estimate r_v: An underestimation of this value, for example, will lead us to overestimate the potential energy in the virial theorem and hence the virial mass obtained from it. Thus, given the density distribution of the universe $\rho(z)$, C96 estimates r_v to be a function of r_{200}, the radius at which the mean interior density is $200\rho_c(z)$, based on analytic models (Gorr & Gunn, 1972) and simulation data (Cole & Lacey, 1996 and Zembrowsky & Carlberg, 1996). The problem is that in some cases, our density will overcome the limiting value of $200\rho_c(z)$, so C96 proposes a superior value of r_{200} of:

$$r_v = r_{200} = \frac{\sqrt{3}\sigma_1}{10H(z)}$$

Where $H(z)$ is the Hubble's constant at a given redshift (in the present work, we'll use $z = \bar{z}$, the cluster's redshift), given by:

$$H(z) = H_0\sqrt{\Omega_m(1+z)^3 + \Omega_k(1+z)^2 + \Omega_\Lambda}$$

Finally, our mass estimation will be given by:

$$M_{200} = \frac{3}{G}\sigma_1^2 r_{200}$$

II. The Data

A. The (2-D) Spectra of Galaxies

The images used to determine the redshifts in the present work where taken by the FORS2 Instrument at Cerro Paranal Observatory. The total data set consists on four masks with two chips each. Each chip contains a science image containing two dimensional spectra of ~ 15 galaxies taken with a exposure time of ~ 1640 secs, five flat-field images and one image containing the two dimensional spectra of the calibration Hg-Cd-He-Ar lamp. An image of a part of the chip science image can be seen in Figure 1. The noise present in the images are mainly cosmic rays that have to be removed in order to extract the one dimensional spectrum. The value of the Gain and the R.O.N. on the images are 1.43 and 3.15, respectively.

B. Data Reduction

B.1 Cosmic rays extraction

The first step to obtain the one dimensional spectrum of each galaxy is to remove the cosmic rays present in

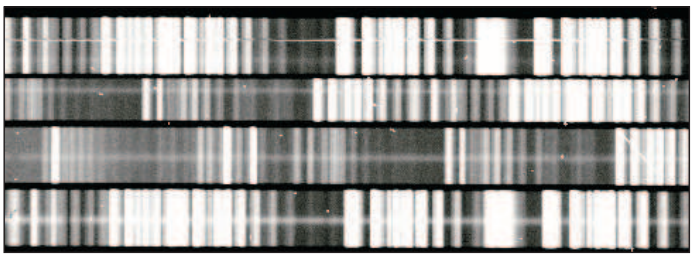

Fig. 1. Section of an image of the chip's image with four spectra taken from different galaxies at the FORS2 instrument (Mask 4, chip 2).

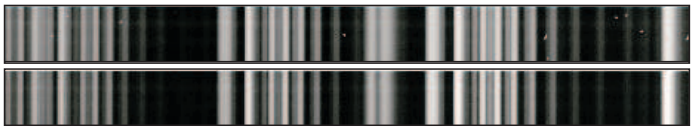

Fig. 2. Same part of a two dimensional spectrum of a galaxy. The comparison before (up) and after (down) the algorithm was applied to the image can clearly be seen.

the image. For this, we used the Laplacian Cosmic Ray Identification algorithm designed by van Dokkum (2001), particularly his IRAF task version `lacos_spec`, which is specially designed for the removal of cosmic rays in spectra. Because the algorithm is based on the shape of the cosmic rays, the image has to be cutted into the individual two dimensional spectrum for each galaxy for the algorithm to work properly. Working with the entire image of the chip removes the lines in the spectra, because the different galaxies are all taken at the same exposure time and hence edges of lines of bright galaxies are confused with cosmic rays.

First, we combined the flat field images using the median. Then, we cutted every spectrum identified visually in the science image, and using the same pixel coordinates cutted the lamp and it's respective (master) flat field image. Each flat field image was divided by it's median value, to avoid obtaining high values when normalizing the science and lamp images and where then used to normalize each column of the science and lamp images by dividing those by the flat field image. With the normalized sciencie images, we ran the `lacos_spec` task with variable `sigclip` parameters (from 15 to 20 in some images: The value depended highly on the S/N ratio on the images). The result before and after applying the algorithm to one of our two dimensional spectrum is shown on Figure 2.

B.2 1-D Spectrum extraction

We used IRAF's task `apall` to extract the one dimensional spectra from our galaxies. To determine the aperture and dispersion axis, we determined the aperture center and background interactively. After that, we fitted a solution to the dispersion axis and finally obtained the non-wavelength calibrated one dimensional spectrum. Using that fit, we extracted the one dimensional spectrum of

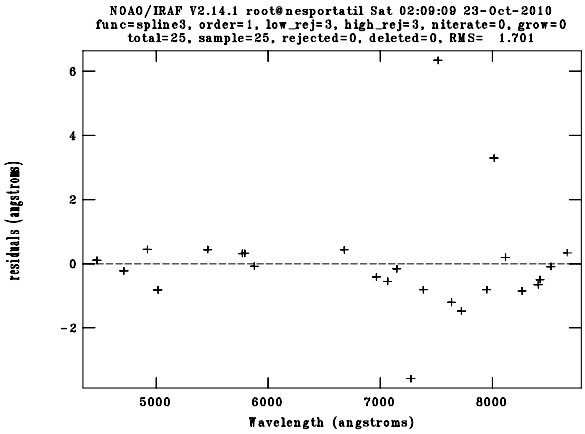

Fig. 3. Fit of the residuals of the pixel/wavelength relation obtained with `identify`, an IRAF task.

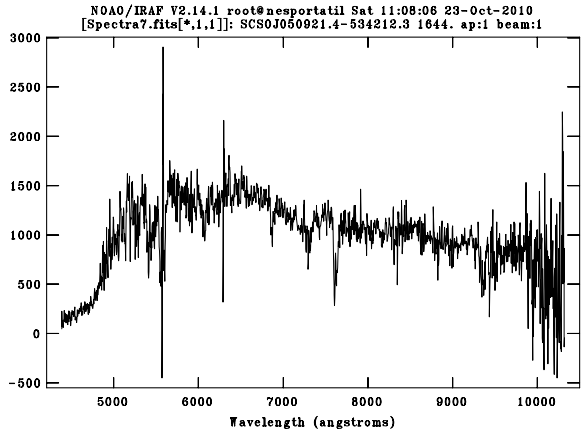

Fig. 4. Calibrated spectrum of a galaxy. We note the sky-emission features of the spectrum at $\sim 5590\AA$ and at $\sim 6300\AA$ in all of our spectra.

our calibration lamps.

For the wavelength calibration of our spectrum, we used a Hg-Cd-He-Ar lamp. We first visually identified some of the lines and then fitted a pixel/wavelength solution using IRAF's `identify` task. A typical fit of the residuals of this relation is shown on Figure 3. We then edited the galaxy spectra headers to asociate each lamp to the corresponding galaxy. Finally, we ran the IRAF's `dispcor` task to obtain our wavelength calibrated spectra. A plot of a calibrated spectrum is shown in Figure 4. Note that it is possible to identify visually the sky-emission lines predicted by Hanuschik (2003) at ~ 5590 $\AA$ and at ~ 6300 $\AA$ in our spectrum.

III. Data analysis

A. Redshift estimation

We use the IRAF's Radial Velocity Package RVSAO to estimate the redshift of our galaxy sample. In particular, the `xcsao` task of the RVSAO package can use both, the

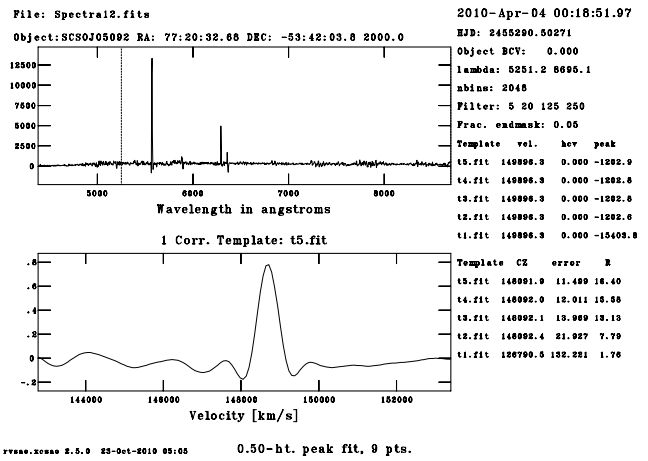

Fig. 5. Spectrum of a galaxy and it's cross-correlation function given by `xcsao` task. The cross-correlation peak is at ~ 0.8.

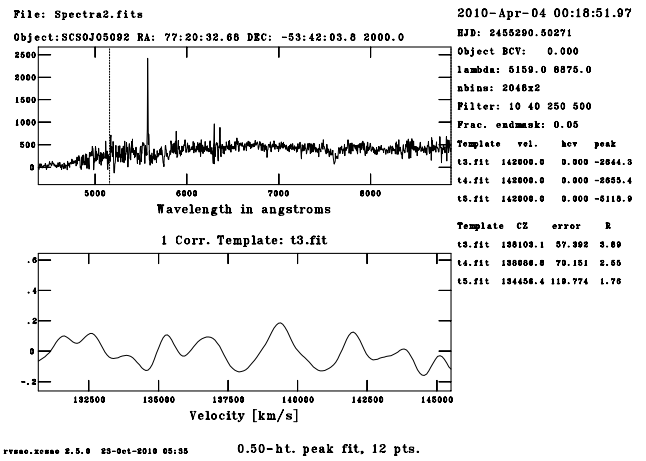

Fig. 6. Spectrum of a galaxy and it's cross-correlation function given by `xcsao` task. Note that it gives no information on the object's velocity.

cross-correlation method proposed by TD79 (described in the Introduction section) and/or the method of observed/-known wavelength relation in the galaxy spectrum (also described in the Introduction section). This is very useful because, as predicted, warned and exemplified by TD79, there are spectra that just can't be correlated with good enough precision (i.e. don't possess symmetric correlation functions and/or a cross-correlation function peak > 0.6, which is mainly because (a) our spectra are not sky-line corrected and (b) the S/N ratio is usually a function of wavelength), so a group of emission/absorption lines must be identified to calculate the redshift. The templates used by the cross-correlation technique where obtained from the SDSS cross-correlation templates[1], where we only used the galaxy ones to correlate our data.

We first estimated the redshift visually by observing the red-shift in the strong Ca H and Ca K absorption lines to be $z \sim 0.45 - 0.46$ in a small sample of our galaxies. Then, we used the SDSS Plate Browser Tool and searched for galaxy spectra in this range, finding that we should also search for Mg, Na, G and H_η absorption lines and the OII emission line. Given this information, we let only this lines to be searched by RVSAO (this also served as a double-check for stars in our spectra: None where found, at least in mask 4, chip 2). An example of a good cross-correlation is given in Figure 5. On the other hand, a poor cross-correlation to a different spectrum is given in Figure 6. However, the absorption lines are very well fitted by the `xcsao` task in the same spectrum, as shown in Figure 7. As we can see, we can use both methods to estimate the object's redshift, which gives us a much better estimate of the object's velocity.

[1] http://www.sdss.org/dr5/algorithms/spectemplates/

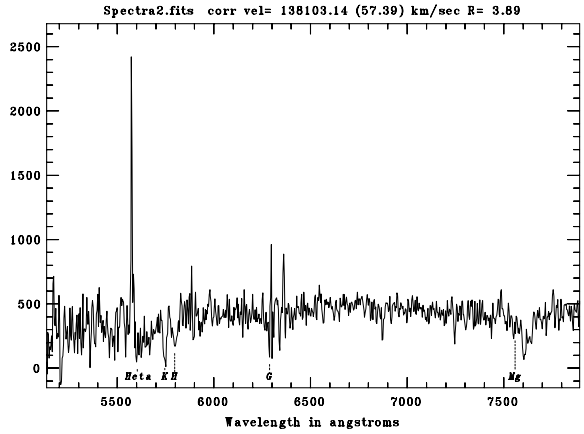

Fig. 7. Spectrum of a galaxy and it's adjusted absorption lines by `xcsao` task.

B. Determination of the Cluster's Members: The cluster's velocity and velocity dispersion

B.1 Deviaton from normally distributed data

Figure 8 shows the radial velocity (cz) distribution for 100 equally spaced bins of our 123 measured galaxy velocities. Following the procedure done by Ferrari et al. (2005), we use the standard iterative 3σ clipping method to eliminate galaxies not belonging to the cluster (Yahil & Vidal, 1977). Only for visualization, Figure 9 shows a plot of the Probability Density Function (PDF) of our 107 remaining cluster members in 50 equally spaced bins after applying the 3σ iteration. It is clearly seen that the distribution deviates from normality (specially at values far from the fitted normal distribution's mean). We are tempted to leave only the central values of our obtained distribution (between ~ 135000 and ~ 142500 km/s) from visual inspection of the data so, for this purpose, we will stay with the result given by the 3σ iteration, but we'll also bring another data set from our data, namely, the results when we

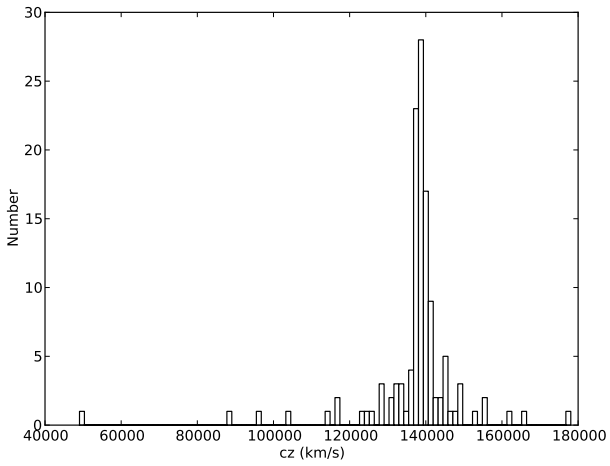

Fig. 8. Histogram obtained from our 123 obtained redshifts. 100 equally spaced bins are made, between 49058.25 and 178076.72 km/s.

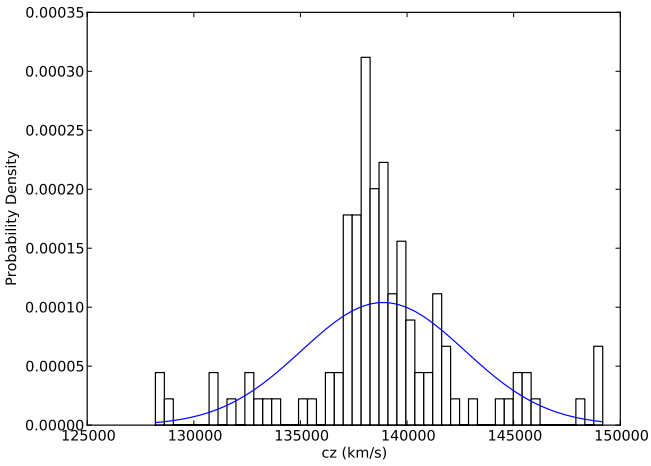

Fig. 9. Probability Density Function for our remaining 107 cluster members. We note that the distribution clearly deviates from normality (blue solid line).

do a 2.6σ iteration. The reasons for this will be clearer in future sections, but suffices to say that between 3σ (99.73 % confidence interval) and 2.6σ (∼99.65 % confidence interval) the result shouldn't (in principle) change much. To see if this is true in our sample, we do $n-\sigma$ iterations to our data from $n=2$ to $n=3$ in bins of 0.01 and compare σ_f, the final sample standard deviation obtained after the iteration. Figure 10 shows how the final sample standard deviation (σ_f) changes as a function of n in our $n-\sigma$ iterations. We can clearly see that after 2.6σ the sample standard deviation changes abruptly, contrary to our intuition about the confidence intervals. Figure 11 shows the PDF of the result after doing the 2.6σ iteration, leaving us with 83 cluster members. The data is also fitted with a normal distribution with the mean and standard deviation of the sample. We note that this PDF also is visually asymmetric. Given the visual inspection of our two PDF's, we suspect that the usual mean and standard deviation are no longer resistant and robust estimators of our sample (Beers et al., 1990, hereafter B90). To show this, we apply D'Agostino and Pearson's test (D'Agostino & Pearson, 1973), which provide us with a 2-tail probability estimation of the normality of our distribution. We simulated 10000 data sets of 107 (83) normally distributed velocities, using the mean and the sample standard deviation of our 107 (83) sample cluster galaxies and calculated the minimum 2-tail probability for each one of them. The order of this minimum probability was $P_{sim}\sim 10^{-7}$ for the 107 (83) normal random simulated variables. Applying the test to our sample data gives a 2-tail probability of $P^{107}_{sample}\sim 10^{-26}$ for the 107 cluster members and $P^{83}_{sample}\sim 0.18$ for our 83 cluster members. We thus conclude that the velocity distribution of our sample of 107 galaxies deviates from a normal distribution, whereas our sample of 83 galaxies has little 2-tail probability of being normally distributed. Therefore, we conclude that we need stronger estimators of the cluster's velocity and the velocity dispersion of the cluster members.

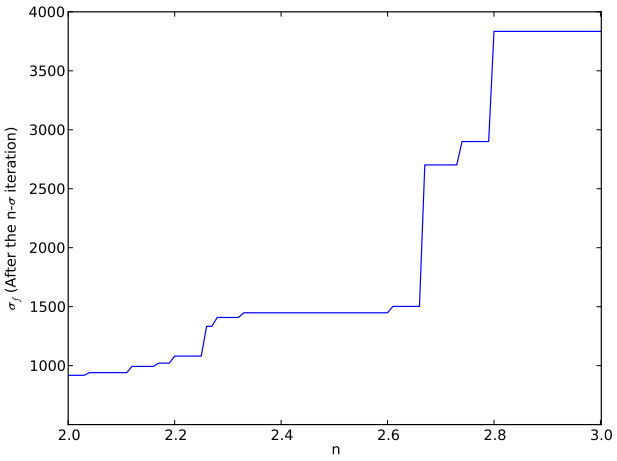

Fig. 10. Results of our $n-\sigma$ iterations from $n=2$ to $n=3$ in bins of 0.01. Our results show that from $n=2.28$ to $n=2.6$ the final sample standard deviation doesn't have abrupt changes. On the other hand, from $n=2.61$ to $n=3$ the sample standard deviation has serius changes, contrary to our intuition about confidence intervals.

B.2 Cluster's radial velocity and radial velocity dispersion

B90 proposes various estimators for location and scale. In particular, we'll take the biweight estimator of location and scale to obtain our mean apparent velocity and velocity dispersion respectively, because of it's superior robustness and resistance. We obtain a mean velocity estimator of $C^{107}_{BI}=138731.495$ km/s, which enable us to obtain the cluster's redshift, $\bar{z}_{107}=0.4627$ for our sample with 107 galaxies. The scale given for this biweight estimator is $S^{107}_{BI}=2716.005$ km/s. For our sample with 83 galaxies, we obtain $C^{83}_{BI}=138744.780$ km/s which enable us to obtain the cluster's redshift, $\bar{z}_{83}=0.4628$. On the other hand, we obtained a scale biweight estimator of $S^{83}_{BI}=1463.748$

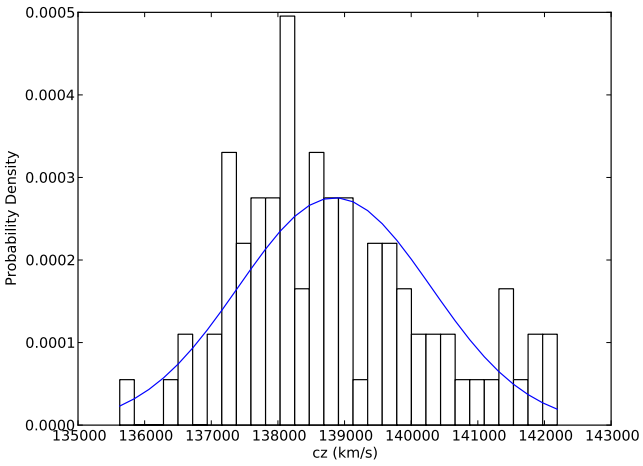

Fig. 11. Probability Density Function for our remaining 83 cluster members after doing the 2.6σ iteration. We note that the distribution deviates visually from normality (blue solid line).

km/s.

To obtain the desired σ_1 velocity dispersion, we must first correct this estimator to the rest frame in the cluster. This is done multiplying by the scale factor $a(t) = (1 + \bar{z})^{-1}$, which finally gives $\sigma_1^{107} = a(t)S_{BI}^{107} = 1857.73$ km/s for our 107 galaxy sample and $\sigma_1^{83} = a(t)S_{BI}^{83} = 1001.19$ km/s for our 83 galaxy sample. To obtain our scale estimator's error, we created an algorithm in the Python Language Code that does the standard bootstrap algorithm (as proposed by B90) with 10000 iterations. Then, we convert our frecuency distribution to a probability density function and integrate it to find the lower and upper $1-\sigma$ errors (68.2% confidence interval). We find the upper error of our 107 galaxy sample to be $\sigma_+ = 231.15$ and the lower one to be $\sigma_- = 221.52$, so our final estimation of the velocity dispersion is $\sigma_1^{107} = 1857.73^{+231.15}_{-221.52}$ for this sample. On the other hand, the upper $1-\sigma$ error found for our 83 galaxy sample is $\sigma_+ = 54.24$ and the lower one is $\sigma_- = 54.98$, so our final estimation of the velocity dispersion is $\sigma_1^{83} = 1001.19^{+54.24}_{-54.98}$ for this sample. We also obtain the errors for the location estimators C_{BI}, obtaining $C_{BI}^{107} = 138731.495^{+125.24}_{-127.45}$ and $C_{BI}^{83} = 138744.780^{+109.20}_{-121.64}$.

B.3 Cluster's mass estimation

For the mass of the cluster, we use the recent WMAP results (Komatsu et al., 2009) which give $\Omega_m = 0.2732$, $\Omega_\Lambda = 0.7268$, $\Omega_k \approx 0$ and $H_0 = 100h$ km s^{-1} Mpc^{-1}. This gives $H(\bar{z}) = 125.71h$, where we used $\bar{z} = 0.462$. Finally, we obtain two different masses for the cluster, depending on the sample of galaxies used:

$$M_{200}^{107} = \left(6.16^{+2.29}_{-2.20}\right) 10^{15} M_\odot h^{-1}$$
$$M_{200}^{83} = \left(9.64^{+1.56}_{-1.58}\right) 10^{14} M_\odot h^{-1}$$

IV. Discussion

A. *Redshift estimation via cross-correlation and visual line identification*

In our data analysis we could test how well the cross-correlation algorithm worked against the visual line identification commonly used. We saw that both methods, in our case, complemented very well. We first noted that trying to fit all the absorption and emission lines that came by default in the RVSAO package gave a redshift estimation of $0.1 \sim 0.2$, and after we realised that the Ca H and Ca K where present in our spectra (therefore realising that the true redshift was about $0.45 \sim 0.46$), decided to choose the lines to be fitted by looking at SDSS spectra in the observed redshift interval. This initial mistake in the redshift estimation was mainly because we didn't substract sky lines present in our spectra, which caused confusion because of the strong sky emission lines detected in the data reduction section. Those emission lines where initially confused by OIII emission lines, which are very strong in redshifts ~ 0.1.

B. *Velocity dispersion of cluster members*

The velocity dispersions for our 107 galaxy sample ($\sigma_1^{107} = 1857.73^{+231.15}_{-221.52}$) and our 83 galaxy sample ($\sigma_1^{83} = 1001.19^{+54.24}_{-54.98}$) have very different values (they don't match, even in a 3σ worst-case scenario), even though the estimator used to derive the dispersions is a very robust and resistant one (i.e. it is designed so that extreme values don't affect it too much). Furthermore, the dispersion in the σ_1^{107} value is way larger than the σ_1^{83} one. By looking at the fact that one was derived using a 3σ criteria (99.73 % confidence interval) and the other by a 2.6σ criteria ($\sim$99.65 % confidence interval), the dispersions are clearly non-correlated and we find that the 24 members eliminated in the 2.6σ iteration weren't actual members of the cluster. Knowing all this information, the argument is now even clearer when we compare Figures 9 and 11.

The velocity dispersion of our cluster (Figure 11) has a very particular shape. It is clearly skewed to the left, which is even clearer if we remember that the normality test for this distribution gaved us a 0.18 2-tail probability. On the other hand, between 141000 and 142000 km/s it appears to be a second maximum. Although a bigger sample (i.e. bigger binsize) is needed to confirm it, if true it may be a sign of a second gravitationally bounded sub-group in the cluster and help in the study of merging galaxy clusters (Ferrari et al., 2005, Bardac et al., 2006, Maurogordato et al., 2008, Okabe & Umetsu, 2008, to name a few) and it would explain the apparent skewness we mentioned in our distribution. This is even clearer if we look at the $1-\sigma$ error values of the velocity dispersion in our cluster, which are almost symmetric.

C. Mass estimation of the cluster

Of the two estimated masses in our analysis, we argumented that the true cluster's mass is the one obtained by using the 83 galaxy sample, i.e. $M_{200} = M_{200}^{83} = \left(9.64^{+1.56}_{-1.58}\right) 10^{14} M_{\odot} h^{-1}$. The cluster appears to be a very massive one in comparison with other studies based on optical estimates of galaxy cluster masses (Girardi et al., 1998, Ferrari et al., 2005), but this can also be a clue of a merging galaxy cluster and hence an overestimation of the cluster's real mass. The argument for this possibility is made clear if we talk in terms of energies: Mass is derived directly from the velocity dispersion and this property is a measure of the equilibrium state of the object. If this object is not in equilibrium (e.g., a group of objects orbit in a prefered direction) we'll overestimate it's energy (e.g. we'll overestimate the velocity dispersion) and hence overestimate it's mass.

V. Conclusions

The use of different methods for the determination of galaxy redshifts (such as visual line identification, automatized line identification and cross-correlation techniques) acted as excellent complementary tools for data reduction. If the calibration of the spectra are good enough (substraction of emission sky lines being the most important feature to be careful with), the cross-correlation technique and the automated line identification method can act as complementary automatized ways of obtaining redshifts of large samples of data.

The biggest problem in our present work was to determine if the 3σ criteria given by Yahil & Vidal (1977) was really the best estimator to define the cluster members. By different statistical tests, we proved that in our case the best estimator was a 2.6σ criteria, so we conclude that it is not always true that a 3σ criteria is the best estimator. One has to be very careful with the choice of σ criteria, and support it with different statistical tests to accept it or modify it, because the 3σ criteria assumes that we have a large sample in which the central limit theorem applies and thus we can approximate our distribution to a normal one. Given our final 2.6σ estimator to determine the cluster members, we find a velocity of the cluster of $v_{clus} = 138744.780^{+109.20}_{-121.64}$ km/s, which gives us a redshift of $z = 0.462^{+0.0003}_{-0.0004}$ from our reference frame.

We finally conclude that our final mass estimation for the galaxy cluster is $M_{200} = \left(9.64^{+1.56}_{-1.58}\right) 10^{14} M_{\odot} h^{-1}$. The comparison of this mass with optical galaxy cluster mass estimations (Girardi et al., 1998, Ferrari et al., 2005) supported even more the question of whether it is really a very massive galaxy cluster or it is an overestimation due to departure from equilibrium (we note that we are not using the same argument twice: Even though it's true that we derived the cluster's mass from the velocity dispersion, let's recall that the velocity dispersion is actually a biweight scale estimator and, by definition, it is not strongly affected by extreme values). This last proposition is supported with the statistical analysis of non-normality of the velocity distribution of the cluster, but requires further study. If true, it could help in the study of merging galaxy clusters (Ferrari et al., 2005, Bardac et al., 2006, Maurogordato et al., 2008, Okabe & Umetsu, 2008, to name a few).

References

[1] E. Hubble, *A Relation between Distance and Radial Velocity among Extra-Galactic Nebulae*, Proceedings of the National Academy of Scienes of the United States of Ameria, Volume 15, Issue 3 (1929) pp. 168-173.

[2] E. Hubble, M. Humason, *The Velocity-Distance Relation among Extra-Galactic Nebulae*, Astrop.J. 74 (1931) pp. 43

[3] W.L. Freedman, B. F. Madore, B. K. Gibson, L. Ferrarese, D. D. Kelson, S. Sakai, J. R. Mould, R. C. Kennicutt, Jr., H. C. Ford, J. A. Graham, J. P. Huchra, S. M. G. Hughes, G. D. Illingworth, L. M. Macri, Peter B. Stetson, *Final Results from the Hubble Space Telescope Key Project to Measure the Hubble Constant*, The Astrophysical Journal, 553 (2001) pp. 47-72.

[4] Andrew J. Benson, *Galaxy Formation Theory*, Physics Reports, 495 (2010) pp. 33-86.

[5] N. Okabe & Keiichi Umetsu, *Subaru Weak Lensing Study of Seven Merging Clusters: Distributions of Mass and Baryons*, Publ. Astron. Soc. Japan, (2008) pp. 1-39.

[6] J. Tonry & M. Davis, *A Survey of Galaxy Redshifts. I. Data Reduction Techniques*, The Astronomical Journal, 84 (1979) pp. 1511-1525.

[7] M. Girardi, G. Giuricin, F. Mardirossian, M. Mezzetti, W. Boschin, *Optical Mass Estimates of Galaxy Clusters*, The Astrophysical Journal, 505 (1998) pp. 74-95.

[8] S. Maurogordato, A. Cappi, C. Ferrari, C. Benoist, G. Mars, G. Soucail, M. Arnaud, G.W. Pratt, H. Bourdin, J-L., Sauvageot, *A2163: Merger events in the hottest Abell galaxy cluster I. Dynamical analysis from optical data*, Astronomy & Astrophysics manuscript no. A2163, (2008).

[9] J. Navarro, C. Frenk, W. Simon, *The Structure of Cold Dark Matter Halos*, The Astrophysical Journal, 462 (1996), p. 563.

[10] F. Gastaldello, D. Buote, P. Humphrey, L. Zappacosta, M. Seigar, A. Barth, F. Brighenti, W. Mathews, *Serendipitous XXM-Newton Discovery of a Cluster of Galaxies at $z = 0.28$*, The Astrophysical Journal, 662 (2007), pp. 923-926.

[11] M. Bardac, D. Clowe, A. Gonzalez, P. Marshall, W. Forman, C. Jones, M. Markevitch, S. Randall, T. Schrabback, D. Zaritsky *Strong and Weak Lensing United. III. Measuring the Mass Distribution of the Merging Galaxy Cluster 1ES 0657-558*, The Astrophysical Journal, 652 (2006), pp. 937-947.

[12] Y. Zhang, N. Okabe, A. Finoguenov, G. Smith, R. Piffaretti, R. Valdarnini, A. Babul, A. Evrard, P. Mazzotta, A. Sanderson, D. Marrone, *LoCuSS: A Comparison of Cluster Mass Measurements from XMM-Newton and Subaru – Testing Deviation from Hydrostatic Equilibrium and Non-Thermal Pressure Support*, The Astrophysical Journal, 711, Issue 2, 1033-1043 (2010).

[13] S. Allen, *Resolving the discrepancy between X-ray and gravitational lensing mass measurements of clusters of galaxies*, Monthly Notices of the Royal Astronomical Society, Volume 296, Issue 2, pp. 392-406 (1998).

[14] Xiang-Ping Wu, *A combined analysis of cluster mass estimates from strong lensing, X-ray measurement and the universal density profile*, Monthly Notices of the Royal Astronomical Society, Volume 316, Issue 2, pp. 299-306 (2000).

[15] Xiang-Ping Wu, *A combined analysis of cluster mass estimates from strong lensing, X-ray measurement and the universal density profile*, Monthly Notices of the Royal Astronomical Society, Volume 316, Issue 2, pp. 299-306 (2000).

[16] H. Y. Shan, B. Qin, H. S. Zhao *Mass discrepancy in galaxy clusters as a result of the offset between dark matter and baryon distributions*, Monthly Notices of the Royal Astronomical Society, Volume 408, Issue 2, pp. 1277-1282 (2010).

[17] C. Ferrari, C. Benoist, S. Maurogordato, A. Cappi, E. Slezak, *Dynamical state and star formation properties of the merging galaxy cluster Abell 3921*, Astronomy and Astrophysics, 430 (2005), pp. 19-38.

[18] M. Takizawa, R. Nagino, K. Matsushita, *Mass Estimation of Merging Galaxy Clusters*, Publ. Astron. Soc. Japan 62 (2010), pp. 951-963.
[19] J.N. Bahcall & S. Tremaine, *Methods for determining the masses of spherical systems. I - Test particles around a point mass*, Astrophysical Journal, Part 1, 244 (1981), pp. 805-819.
[20] P.G. van Dokkum, *Cosmic-Ray Rejection by Laplacian Edge Detection*, PASP, 113 (2001), p. 1420.
[21] R.W. Hanuschik, *A flux-calibrated, high-resolution atlas of optical sky emission from UVES*, A&A. 407 (2003), pp. 1157-1164
[22] A. Yahil, N. Vidal, *The Velocity Distribution of Galaxies in Clusters*, Astrophysical Journal. 214 (1977), pp. 347-350
[23] D'Agostino, R.B. and Pearson, E.S., *Testing for departures from Normality*, Biometrika. 60 (1973), pp. 613-622
[24] E. Komatsu, J. Dunkley, M.R. Nolta, C.L. Bennet, B. Gold, G. Hinshaw, N. Jarosik, D. Larson, M. Limon, L. Page, D. Spergel, M. Halpern, R. Hill, A. Kogut, S. Meyer, G. Tucker, J. Weiland, E. Wollack, E. Wright, *Five-Year Wilkinson Microwave Anisotropy Probe Observations: Cosmological Interpretation*, The Astrophyiscal Journal Supplement, 180, Issue 2 (2009), pp. 330-376